Vascular Atlas Formation Using a Vessel-to-Image Affine Registration Method

Dini Chillet[1,2], Julien Jomier[1], Derek Cool[1], and Stephen R. Aylward[1]

[1] Computer-Aided Diagnosis and Display Lab
The University of North Carolina at Chapel Hill, Department of Radiology
27510 Chapel Hill, USA
{aylward,jomier}@unc.edu
[2] Ecole Superieure de Chimie Physique de Lyon
69100 Lyon, France
dini.chillet@cpe.fr

Abstract. We have developed a method for forming vascular atlases using vascular distance maps and a novel vascular model-to-image registration method. Our atlas formation process begins with MR or CT angiogram data from a set of subjects. We extract blood vessels from those data using our tubular object segmentation method. One subject's vascular network model is then chosen as a template, and its vascular distance map (DM) image is computed. Each of the remaining vascular network models is then registered with the DM template using our vascular model-to-image affine registration method. The DM images from the registered vascular models are then computed. The mean and variance images formed from those registered DM images are the vascular atlas.

In this paper we apply the atlas formation process to build atlases of normal brain and liver vasculature. We use Monte Carlo simulations to demonstrate the reliability of the underlying registration method. Additionally, we explain the clinical potential of those atlases and conduct z-score analyses to compare individuals with the atlases to detect abnormal vessels.

1 Introduction

Much research has focused on generating tissue atlases. Significantly less time has been spent on formimg vascular atlases. Nevertheless the interest exist, indeed if we took all of the blood vessels in the human body and laid them out in one line, the line would be approximately 100,000 miles long, and it has been shown that vessels located nearby a tumor presents "abnormal" attributes such as radius, concentration, and tortuosity [1]. Similarly, strokes are often caused by the presence of aneurysms, which are dilated blood vessels inside the brain; and a vascular atlas could ease the detection of such abnormals vessels. Furthermore, we hypothesize that vascular atlases might even aid in diagnosing mental disorders, such as psychophrenia, that have a strong genetic component. In particular,

researchers have shown that intra-cranial vasculature actually forms prior to and potentially drives the development of the brain's tissues [2]; a vascular atlas may provide a more direct measure of the genetic component of such mental disorders.

In our previous research, a vascular model-to-image rigid registration method has been shown to be reliable and accurate [5]. In that research, the aim was to register the vasculature of the same patient from different scans taken at different times, e.g., MR scans before, during, or after a surgical intervention. In the following work, we are registering vasculature from different subjects; a rigid transform is clearly not sufficient, and inter-patient vascular network variability confounds the use of standard model-to-model and image-to-image match metrics.

In this paper, we present our method for making vascular atlases using a vascular model-to-image affine registration method and a distance map (DM). A DM is an image in which each voxel's intensity corresponds to the expected distance to the nearest vessel. By registering an individual's vascular model (cf fig. 1) with a DM, correspondence issues due inter-patient vascular network variability are eliminated. Thus, for a group of subjects we register each subject's vascular network with the DM (the DM is initially defined using one subject's vascular network). We then compute the DMs of those registered vascular networks; the mean and variance images of those DM forms the atlas. We present results from Monte Carlo simulations that show vascular model-to-image registration using a DM is reliable and therefore the resulting atlases and their measures are stable. Because of this stability our vascular atlas can be used to detect vascular anaomlies within an individual and to quantify vascular network differences between populations, e.g., to detect schizophrenia.

Our method has been applied to form atlases of normal brain and liver vasculature, and basic statistical analyses have been conducted. Specifically, we computed the z-score for all the subjects to show that the atlases well represent their populations.

2   Method

2.1   Blood vessels modeling and extraction

The model chosen to represent a vessel is a centerline, constitued of a set of points. In our N-Dimensional data, each points has as components:

x_i ($x_i \in \Re^N$)	Spatial position
r_i	Radius
m_i	Medialness; a measure which indicate how well the vessel section is differentied from the background[3]

Images issued from CT or Mangnetic angiogam scans can be used for our method. Blood vessels are the bright voxels in these images and are extracted using the dynamic scale intensity ridge and radius estimation method detailed in [3]. The process includes three steps: (1) selecting a seed point inside or nearby a vessel, (2) traversing the centerlines of the tubes as intensity ridges, and (3) estimating the radius at each ridge point.
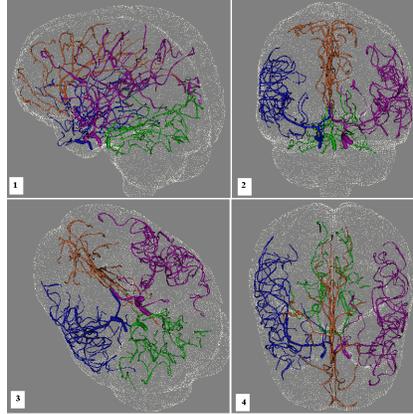
Fig. 1. Brain vasculature and tissue enveloppe: from four differents points of view 1)left side , 2)front, 3)bottom 4)top. Those are blood vessels from a normal subject got from a MR angiogram with our tubular extraction (cf section 2.1

2.2   Compute distance map

The computation of the DM gives an image, where the intensity value at each voxel is the distance from the closest vessel. That calculation is done using the algorithm developed by Danielsson [4]. The intensity of the DM is also inverted to get the Inverted Distance Map(IDM) in which the brightest pixels are nearest a vessel, and the intensity decrease further away from a centerline. This produces an image of "blurred vasculature." This blurriness is illustrated in fig.2.
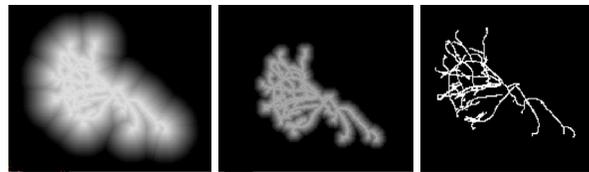

Fig. 2. Inverted Distance map(IDM) of a vasculature from the liver. The point of view is axial. On the *left* picture, a threshold is applied to show the intensity fall-off near the centerlines. The blurred nature of the DM vasculature network is obvious. The *middle* image is the same IDM, with a higher threshold; only the voxels close to a centerline point have an intensity value $\neq 0$. The *right* image depicts the vessel centerlines.

2.3   Vessel-to-image Affine Registration

In registration the critical parts are the transform, the optimization method, and the match metric. The transform in our atlas formation system is a basic affine

transfom. It has a 12 dimensional parameter space. The *one-plus-one evolutionary optimizer* has been developed by Styner and al. [8]. It uses a normal distribution randomly walk in parameter space to find a global maximum and updates the covariance matrix of the normal distribution to converge to a solution. The *vessel-to-image match metric* measures how well a affine matrix $\mathbf{R}$ and an offset vector $\mathbf{o}$, applied to a vascular model, align that model with an image. For our system, the metric is maximal when the centerline points x_i of the model map to the scaled brightest pixels in the IDM.

$$F(\mathbf{R}, \mathbf{o}) = \frac{1}{\sum_{j=1}^{n} w_j} \sum_{i=1}^{n} w_i \mathbf{I}_{kr_i}(\mathbf{R}x_i + \mathbf{o}) \tag{1}$$

Therefore, the metric depends on the centerline sampling (x_i and n) and the scale (kr_i) of the Gaussian used to blur the IDM (reducing the influence of the noise [7]). Additionally, the parameter w_i is used to weight samples depending on their radius r_i; weighting increases from $w_i = 0$ at $r_i = 0$ to an asymptote of $w_i \cong 1$ at $r_i \cong 3$.

$$w_i = \frac{2}{1 + e^{-2r_i}} - 1 \tag{2}$$

Those parameters have been analysed in [5] and [6].

2.4   Atlas formation

The processing pipeline of the atlas formation can be divided in three steps. First, among the different vascular networks (V_i), one is chosen as a template. The chosen network's IDM is computed (cf section 2.2) to get $IDM_{template}$. The remaining vascular networks are then registered with $IDM_{template}$ using the vessel-to-image affine registration method (cf section 2.3). Those registrations provide n transform parameters (T_i), which are n translation vectors and n affine matrices.

Second, the parameters (T_i) are applied to each IDM_i to transform them into a common coordinate system. Thus, each IDM_{Ti} is aligned with the template DM_T.

Third, the mean and the variance images from the (IDM_{Ti}) are calculated to form the atlas. The entire pipeline is shown on figure 3.

3   Results

Three tests were conducted using liver and brain data. These tests quantify (1) the reliability of the affine registration process for vascular model to DM registration across patients, (2) the generalization ability of the atlases to accept subjects from the same population, and (3) the ability of the atlases to discriminate subjects from different populations.

Monte Carlo simulations were used to quantify the reliability of the affine registration process. We repeated 100 registrations of a vascular model from one
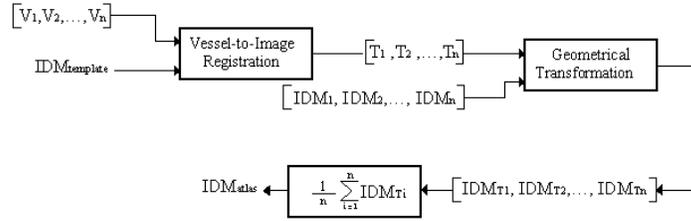
Fig. 3. Processing pipeline of the atlas formation

patient's liver (cf fig. 4) with another patient's IDM. For each registration, the vascular model was initially displaced by an offset up to ± 10 voxels (1 cm) and a rotation up ± 0.15 rad (8.5 degrees). The vascular networks of the patients were very different in terms of the number and the position of the vessels in their liver.

The liver vasculature is comprised of two venous systems: the portal system (shown as bright vessels in fig.4) brings blood into the liver; the blood is then transported out of the liver by the hepatic system (shown as dark vessels in fig.4). Our first tests led us to separate the vasculature of the liver in order to form two different atlases, one for the hepatic and the other for the portal system. Indeed, for some subjects, these networks were so different that it was impossible to match both hepatic and portal vessels together. Separating these systems resulted in very repeatable registrations (discussed next) and perhaps will allow the atlases to detect more subtle venous system dependent anamolies such as accessory renal veins.
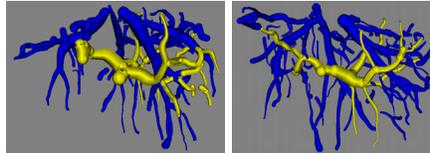

Fig. 4. Liver030(left) and Liver032(right) issued both from normal subjects. The hepatic system appears in dark and the portal in bright. The vasculatures differentiate a lot by the number and the location of the vessels

Results from the Monte Carlo simulations are given in fig.5 and show that only five of the one hundred instances failed to converge to a consistent solution for the hepatic system and only eight failed for the portal system. The stastistics, below the two plots on the fig.5, indicate a low standard deviation for the offset, even for the wide range of initial mis-registrations used. Monte Carlo simulations were also conducted using intra-cranial vascular networks from two patients; there was no need to split the vascular trees within the brain; the repeated

registrations of the complete intra-cranial networks were as reliable as those of either of the venous systems in the liver. The second analysis of the atlas focused
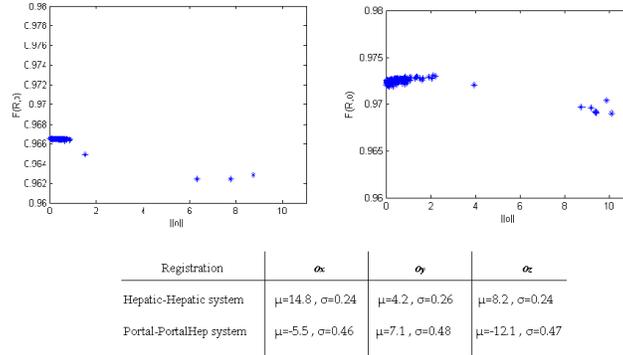

Registration	o_x	o_y	o_z
Hepatic-Hepatic system	μ=14.8 , σ=0.24	μ=4.2 , σ=0.26	μ=8.2 , σ=0.24
Portal-PortalHep system	μ=-5.5 , σ=0.46	μ=7.1 , σ=0.48	μ=-12.1 , σ=0.47

Fig. 5. Results of the Monter Carlo simutation for the registration of the hepatic and the portal system. The two plots show, for the 100 instances,(x-axis) the euclidean distance from the offset **o** to the average value of **o** -versus- (y-axis) the metric's value. The *left* plot comes from Hepatic-Hepatic registration, and the *right* one from Portal-Portal registration. Both reveal few non-optimal registrations (on the right) with smaller metric's value. The table shows that for each translation, after rejecting the non-optimal registrations, in both registrations the standard deviation is low which prove a good constancy of the registration.

on its ability to describe the population from which it was formed. We formed an atlas from nine MR angiogram of normals subjects and then computed the fit between those individuals and the atlas. To quantify the fit, we computed the voxel-by-voxel *z*-scores for all the subjects using the mean and variance estimates of the atlas. The z value indicates by how many standard deviations σ the intensity value at a voxel of an individual's DM differs from the mean intensity value μ at that voxel as capture by the atlas.

$$z_i = \frac{x_i - \mu_i}{\sigma_i} \tag{3}$$

x_i being the intensity of the voxel i, μ_i and σ_i being respectively the mean and the standard deviation in the atlas at the same position. A mask is used to limit z-score calculation to the volume covered by an individuals scan. Having a z-score value at each voxel allows local statistical anomalies to be detected. Calculating the histogram of z-scores within an individual's scan supports global comparisions across individuals as well as the verification that the population is well represented by a normal distribution.

The z-score distributions for the individuals that were used to form the atlas are given in fig.6. These results indicate that the atlas represents the population

well, and the population has a normal distribution; however, an abnormal distribution of z-scores was measured in one individual. A review of that individual's anatomic and vascular data suggest a small physical deformation.

As a further test of how well the atlas represents the population, a 10th normal subject was registered with the atlas and given z-scores. This individual was also considered to have normal vasculature by a neurosurgeon but was not used to form the atlas. The z-scores for this individual are also indicated in fig.6. Those scores are well correlated with the scores from the individuals who were used to form the atlas. This indicates that the atlas does effectively represent the population. The third validation of the atlas focused on its ability to dif-

Percentage of voxels basing their z-score	$z \leq 0.4\sigma$	$z \leq 1\sigma$	$z \leq 2\sigma$
Normal001	61%	93 %	100 %
Normal002	43%	98 %	100 %
Normal003	46%	86 %	93 %
Normal004	47%	98 %	100 %
Normal005	30%	89 %	99 %
Normal006	47%	96 %	100 %
Normal007	44%	94 %	100 %
Normal008	51%	96 %	99 %
Normal009	49%	99 %	100 %
New Normal	51%	97 %	99 %
AVM Case	10%	36 %	80 %

Fig. 6. This table show percentage of voxels, for different subjects, whom the $z$value is under 0.4, 1 and 2 standard deviation of the atlas. AVM was a patient affected by a Arterio Venous malformation six months after his surgery. The percentage show that normal subjects are well represented by the atlas, but a subject , who differentiated from the population, is flagged.

ferentiate an individual that belongs to a different population. This was tested using the MRA data from an individual with an arterio-venous malformation. That data was registered with the atlas, and corresponding z-score values were calculated. Those results are also reported in fig.6 and illustrated in fig.7 The AVM manifested as both global and localized anomalous z-score values.

4   Discussion and Conclusions

In this paper we introduce the concept of a vascular atlas formed by registering vascular models. The basis of the registration is the calculation of a vascular distance map and the application of a vascular model-to-image affine registration technique.

The application of our intra-patient vascular registration and atlas formation method is demonstrated using portal venous networks, hepatic venous networks, and intra-cranial vasculatures. Monte Carlo experiments quantify the reliability
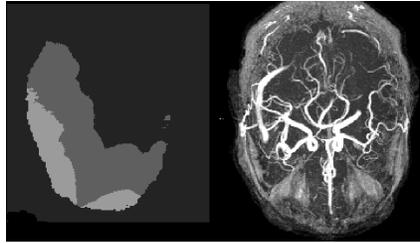
Fig. 7. Image on *left* shows z-score values,z=0 , z=1 and z=2 for respectively black, grey and white voxels. We could suppose some anomalies on the left side of this brain, which is verify the MR angiogram on the *right* and the big vessel

of the registration process for liver and intra-cranial networks. Furthermore, the intra-cranial atlas is able to correctly differentiate the vascular network from a healthy individual from a vascular network from an individual with an arterio-venous malformation. In the latter case, the location of that lesion within the individual was also correctly identified via the application of the atlas.

Much additional work remains to truly validate and demonstrate the utility of vascular atlases. However, this paper represents an important first step in that process. Future work will focus on the application of these atlases to identify vascular fill regions to help predict the development of collatoral flow during recovery from strokes. There is also great potential in the application of the intra-cranial atlas to the early detection of mental disorders that have strong genetic components.

References

1. Bullit E, Gerig G, Pizer S, Lin W, Aylward S, "Measuring Tortuosity of the Intrac-erebral Vasculature from MRA Images" accepted IEEE-TMI pending revision.
2. Seydel C "Organs Await Blood Vessels'Go Signal" in Science Vol 293 September 2001, p 2365
3. Aylward S, Bullit E, "Initialiation, Noise, Singularities, and Scale in Height Ridge Traversal for Tubular Object Centerline Extraction" in IEEE Transactions on Medical Imaging, Vol 21,No2 February 2002
4. Danielsson P.E., "Euclidean distance mapping" in Computer Graphics and Image Processing, 14, 1980, pp. 227-248.
5. Aylward S, Jomier J, Weeks S, Bullit E, "Registration of Vascular Images" in International Jounal of Computer Vision, March 2003, p15.
6. Aylward S, Weeks S, Bullit E, "Analysis of the Parameter Space of a Metric for Registering 3D Vascular Images " MICCAI 2001,p8
7. Lindeberg T,"Scale Space Theory in Computer Vision" in Kluwer Academic Publishers, Dordrecht, Netherlands 1994
8. Styner M, Gerig G, "Evaluation of 2D/3D bias correction with 1+1ES-optimization" in Technical Report BIWI-TR-179